

Experimental research and finite element analysis on Behavior of Steel Frame with Semi-rigid Connections

Wang Xinwu
Department of Civil Engineering
Luoyang Institute of Science and Technology
Luoyang 471003, China
Wxw1971@263.net, wxw197100@sina.com

Abstract: - Most steel beam-column connections actually show semi-rigid deformation behavior that can contribute substantially to overall displacements of the structure and to the distribution of member forces. Steel frame structure with semi-rigid connections are becoming more and more popular due to their many advantages such as the better satisfaction with the flexible architectural design, low inclusive cost and environmental protect as well. So it is very necessary that studying the behavior of those steel frame under cyclic reversal loading.

Three full-scale specimens of angles steel using H-section members had been conducted. The specimens were subjected to cyclic reversal loading simulating earthquake effects on a steel moment-resisting force. Rotational stiffness, the carrying capacity and ductility of top-seat and web angles connections are analyzed. It is concluded that angles connections can possess the relative high stiffness, strength and excellent ductility as moment-resisting components in the seismic design of frames.

At the same time, on the basics of connections experiments the experiment research on the lateral resistance system of steel frame structure has been completed. Two one-second scale, one-bay, two-story steel frames with semi-rigid connections under cyclic reversal loading. The seismic behavior of the steel frames with semi-rigid connections, including the failure pattern, occurrence order of plastic hinge, hysteretic property and energy dissipation, etc, was investigated in this paper. Some conclusions were obtained that by employing top-seat and two web angles connections, the higher distortion occurred in the frames, and the internal force distributing of beams and columns was changed, and the ductility and the absorbs seismic energy capability of steel frames can be improved effectively.

Key words: semi-rigid connection, cyclic reversal loading, hysteretic property, finite element analysis, steel frame

1 Introduction

Beam-to-column connections are integral element of a steel frame, and their behavior affects its overall performance under loading. Vulnerability of welded moment connections in steel moment-resisting frames subject to severe cyclic loading was demonstrated during the 1994 Northridge Earthquake and 1995 Kobe earthquake[1][2]. Since then, a lot of connections have been proposed for the retrofit and the new design of steel moment frames in high seismic areas. One of the proposed connections is top-seat and two web angles connection, many studies show that this connection possess the relative high stiffness, strength and excellent ductility as moment-resisting components in the seismic design of frames[3][4][5].

This paper presents an experiment for steel frames with top-seat and two web angles connections. The

aims are studying the failure pattern, occurrence order of plastic hinge, hysteretic property and energy dissipation of steel frames. In this paper, in terms of the experimental of steel frame structure, the relations of each component of steel frame structure system are discussed. Based on above experimental achievements, the nonlinear finite element computations of one model is carried out here. The load-deflection relation curves, the stress contours under yield load and ultimate load of this model are obtained. It demonstrates that the computing results coincide with the experimental over favorably.

The experimental and finite element computational research shows that this steel frame with top-seat and two web angle connection can improve the ductility of steel frame and possess significant extent lateral resistant rigidity.

2. Experiment Program of Connections

2.1 specimens design

In the design of moment-resisting frames under severe lateral loads, it is reasonable to assume that the points of inflection are located at the mid-span of the beams and the mid-height of the columns. A simple cantilever type beam-column connection, such as the one shown in Fig.1, was chosen as the specimen for this study. The cantilever length represents approximately one-half the length of typical beams in a moment-resisting frame. For simplicity of testing, no attempts were made to simulate axial force in the column. Attention was mainly concentrated on the study of the behavior of the connection itself.

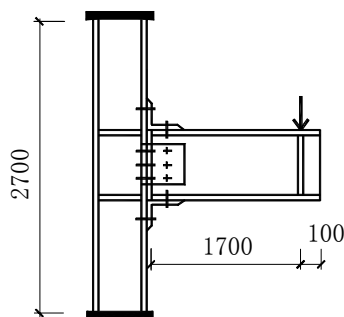


Fig:1 Typical top-seat and web angles connection

The material used for three test specimens including beams, columns, continuity flange stiffeners, top-seat and web angles was in accordance with Q235 steel. Beams and columns were manufactured with rolling H steel. The sizes of beam and column were H300×200×8×12 and H200×200×12×12 respectively. The high tensile bolts used are specified as 20mm diameter, grade 10.9. They were full preloaded according to the China Code. The contacting surfaces between connections components were treated according to China steel design code (GB50017). An average value of the cyclic friction coefficients measured from the cyclic tested was about 0.40.

The main geometrical dimensions are indicated in the table 1.

Table1
Details of the test connection

Specimen	Top-seat angles Size(mm)	Column flange stiffener
JD1	110×12×12	yes
JD2	140×16×14	yes
JD3	140×16×14	yes

2.2 testing apparatus and the measurement setup

All specimens attached through the connection to be test to a “rigid” counter-beam, as shown in Fig.2. The loads are applied to the free end of the specimen by means of a device that transfers horizontal forces only. Testing conditions hence approximate quite closely the case of beam-column joints with negligible column deformability.



Fig2: general view of test arrangement

For monitoring the actuator load, load transducers was loaded in the front of jack. The load transducer was calibrated after each test on a multipurpose test machine. For measuring the connections rotation, electron centigrade instrument was used. The curves of connections rotation and the load were drawn by X-Y function enregistering instrument. Strain gauges were used to monitor the onset of beam flange local bucking and to determine initial yielding of the beams.

All date from strain gauges and transducers were scanned by a multi-channel DH3815 scanner system. The readings were recorded using a microcomputer system.

2.3 loading sequence

To simulate seismic forces the test specimens were subject to a quasi-static cyclic loading. The loading history may be considered one of the most important factors affecting the significant of cyclic tests.

Before reaching the yield point, an individual specimen was first subjected to two load cycles of 20% the expected yield value, then the load was increased 20% the expected yield value and the two load cycles was also adopted. The load was then increased until the initial beam yielding was recorded by the strain gauges or the apparent turning point was turned out in the curve of connection $M-\phi$. Then for subsequent loading cycles, the rotation of connection was incrementally increased by the yield rotation up to the failure of connections. The models of the failure of connections included top and seat angles fracturing, local flections of column flange and the looseness of bolts. In reaching either of failure modes, the test would be terminated. A typical loading routine is presented in Fig.3.

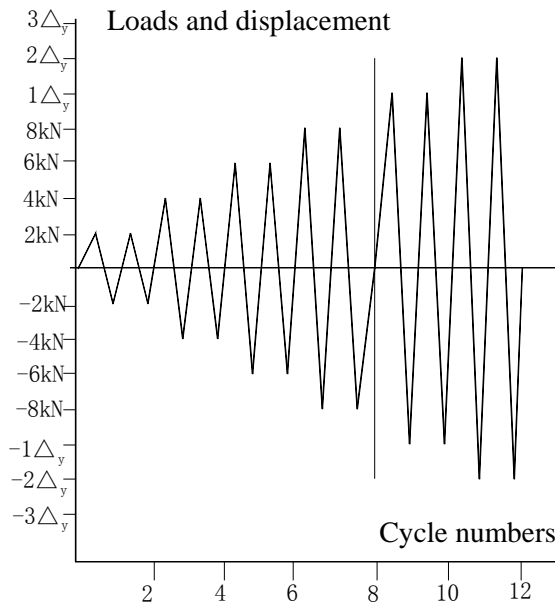
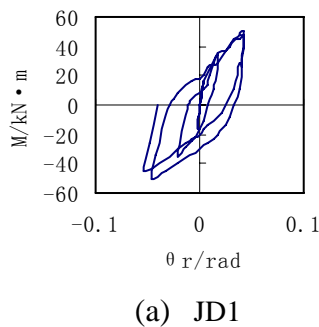


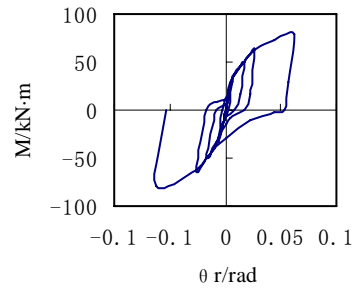
Fig3: actual loading routine of specimens

2.4 Experimental Results and Disucssion

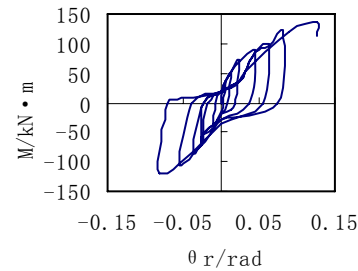
The connection's rotation was the result of top-seat and web angles and column flange deformation and bolt extension. No panel zone deformation was observed, since the column flange stiffeners were designed. Fig.4 showed the moment-rotation hysteretic curves for connection JD1, JD2 and JD3 respectively. As can be observed, all the connections showed stable hysteretic behavior up to the fracture of the connections. In the latter cases, significant degradation occurred in the connection strength after severe distortion and/or crack initiation developed. During latter cycles of the test severe distortion to the column flange was observed. It was evident that column distress could have been avoided with the use of column stiffeners. Failure of the specimen was attributed to severe distortion of the flange of top-seat angles.



(a) JD1



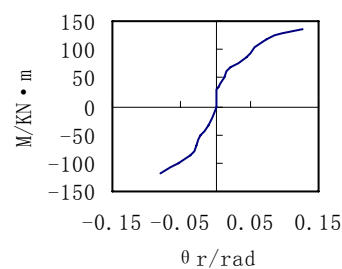
(b) JD2



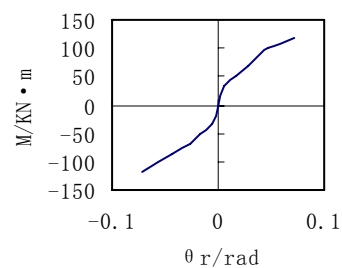
(c) JD3

Fig4:hysteretic curves for specimens

Fig.5 were the envelop of the cyclic response of JD1, JD2 and JD3 respectively. The relations of moment and rotation were outlined. The line relations of moment and rotation were showed in the initial phase and the phase was very short. With increasing the load, the non-line relations of moment and rotation became very apparent. The fluctuating phenomenon of the relations was revealed. The main reason was that the bolts lost their pretension forces significantly in the later stage of loading.



(a) JD1



(b) JD2

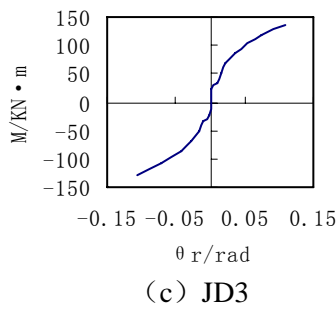


Fig5: Envelope of the cyclic response of specimens

In seismic design, cyclic energy dissipation is of great important, since it expresses the ability of the members and their connections to dissipate earthquake input energy. Generally, sufficient energy dissipation without substantial loss of strength and stiffness constitutes desirable behavior for beam-column subassemblages[3][4][5]. It was confirmed that most of the energy was dissipated in the flange of top-seat angles while the column and web angles participated a little in the energy dissipation process in this test.

The main parameters that describe a connection’s behavior are (1) the connection yield moment, M_y , (2) the initial stiffness of the connection, R_0 , (3) the connection strength, M_u and (4) the connection rotation capacity (i.e.ductility), θ_u . Table 2 shows these parameters for some of the tested specimens. As expected, the initial stiffness of a connection increases as the top-seat angles flange thicknesses increase. This is evident when connections JD1 and JD2 are compared where the column flange thickness differ, while the stiffness of JD2 is greater than that of JD1 because of the former’s greater top and seat angles thickness.

Table2
Joint capacity and ductility

Specimen	R_0	M_u	θ_u	μ_ϕ
JD1	0.71	124.67	0.0788	5.5
JD2	1.03	136.01	0.1097	5.0
	1.16	136.51	0.1265	5.6

R_0 the initial stiffness of connections, $10^4 KN \cdot mrad^{-1}$

M_u maximum moment of connections, $KN \cdot m$

θ_u maximum rotation of connections, rad

μ_ϕ the ductility coefficient of connections $\mu_\phi = \theta_u / \theta_y$

2.5 Conclusions

Based on the experiment work, the following preliminary conclusions and design code

implications can be made about beam-column top-seat angles connections.

(1) All two tested connections showed degradation in stiffness with load cycles due to diminished bolt pre-tension forces and inelastic deformations. Pre-tension forces in all the bolts showed degradation with repeated load cycle. The drop in the pre-tension force continues with increasing the load. To ensure that the bolts do not fail and do not lose their pre-tension forces significantly even during moderate earthquake excitation, it is suggested that the bolts be designed to sustain a force corresponding to beam moment of 1.3Mp.

(2) In all the tests, the connections were not able to sustain moment higher than the beam’s nominal plastic moment capacity. The main reason was that the stiffness of top-seat angles was too weak.

(3) If the stiffeners of the column flange were designed, the most possible failure mode is the fracture of top or seat angles.

(4) because of web angles, these connection’s yield moment were higher than top-seat angles connection’s yield moment, the main reason was that the web angles restrict the deformation of connections.

(5) Most of the energy was dissipated in the flange of top and seat angles while the column participated a little in the energy dissipation process.

(6) When properly designed and detailed, the top-seat and web angles connection, which can provide reasonable strength, stiffness and adequate ductility, can be considered suitable for moment-resisting frames in areas of high seismicity.

3. Experiment Program of Frames

3.1 specimens design

The specimens were designed according to the height of common buildings, the span of columns, the section size of beams and columns, and considered the reduced scale of one-second. The span was 2.4m and the height was 1.4m. Two one-second scale, one-bay, two-story steel frames with semi-rigid connections specimens shown in Fig.6. The material used for two test specimens including beams, columns, continuity flange stiffeners, was in accordance with Q235 steel. Beams and columns were manufactured with rolling H steel. The sizes of beam and column were H200×100×6×8 and H150×150×7×10 respectively. The beams and columns of specimens were taken from the same rolling H steel of one batch. the proportion of chord width and thickness was $b/t = 11.75$, and the proportion of web plate height and

thickness was $h_0/t_w = 30.67$, according to China steel design code(GB50017-2003). To keep accordant, all specimens were made and installed by the workers of the same passel in the same manufactory. The high tensile bolts used are specified as 20mm diameter, grade 10.9. They were full preloaded according to the China Code. The contacting surfaces between connections components were treated according to China steel design code (GB50017). An average value of the cyclic friction coefficients measured from the cyclic tested was about 0.40. The main geometrical dimensions are indicated in the Table 3.

Table3 Details of the test connection

Components	Section aera (cm ²)	Section Inertia	
		I _x	I _y
column	40.55	1660	564
Beam	25.57	1880	134

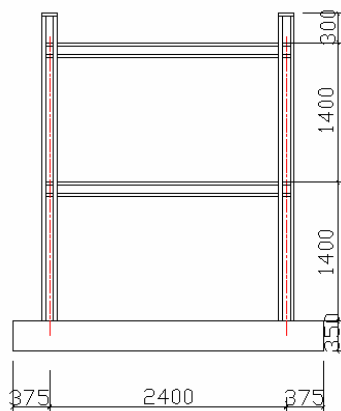
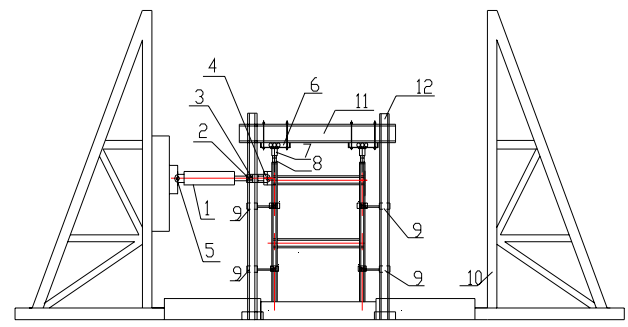


Fig 6 steel frame specimens

3.2 Experimental equipment

As Fig.7 and Fig.8 shown, connections between frame specimens and ground beam were designed into fixed support bearing according to structure requirement. By using channel composed beam and ground bolts to fix the ground beam into the geosynclines of experimental frame to make the bottom firm. By determined in the experimental process of the three-bay steel frame, the maximum displacement of the ground beam was 0.1mm, and the minimum displacement was 0.05mm, which were basically conform to the condition of fixed end. The experiment was carried on the static platform in the structural lab. Little sand was paved on the top of frame ground beam and platform, and was fixed by four bolts.

On the top of the frame column, two hydraulic jacks with anti-edge beams and rolling axletrees linked to the rigid frame were used to apply 80KN axial loads, which was remained unchanged during the test as far as possible. It should be noted that because the horizontal displacement of the steel frame was larger, the top axletrees with a larger rolling scope were required, which was expected to be reached ± 250 mm. By using the tension and compression jack fixed on the counter force shelf, the reciprocating horizontal load was applied on the centre of the top beam of framework. To avoid the framework appearing out-plane instability in the course of the test due to the vertical and horizontal load was not in the same plane, rolling axletrees in the half height of each story corresponding to the frame of the two sides were set up in order to restrict the out-plane deformation of the frame columns. In addition, during imposing the vertical load, observing the strain value of the column footing was observed to estimate if the vertical loads were on the situation.



1,7 jack 2,4,5 connecting fitting 3,8 transducer 6 axletree bearing loading equipment 9 out-of-plane bracing 10,11,12 Counterforce stand

Fig 7 experimental loading equipment



Fig 8 the actual loading equipment

3.3 Type of loading

In order to truly reflect the impact of vertical load, the vertical load must meet the following two points: first vertical load should be able to move together with the framework column, and always maintain a role in the direction of vertical second the action position of vertical load have to keep fixedness during the distortion of test piece. In order to meet the two requirements on the top of each vertical jack finishing with specialized production line installations were set, including roller-box clean wide 300 mm, with 4 rollers whose diameter are 80 mm. Roller was installed in contact with anti-edge-beams at the bottom through the bearings device, when the vertical loads imposed upon freedom of movement, so that the mobile hydraulic jack into the rolling, rolling friction and friction than other sports to small. Measured by the simple, two-way friction roller is about 2 percent, when measured only have a one-way friction, and its value to about 1 percent, therefore, hydraulic jacks in the process of moving caused by the friction can be ignored in practice. Taking into account the jack is a part of the roof-hinged device, thus there are sufficient grounds to believe that the mobile hydraulic jack is moving in parallel. Thus the two requirements also will be met, which are proved in this test.

Examination of the vertical load through two simultaneous jack from a high pressure pump and controlled by hydraulic relief valve control, pressure sensors used by resistance strain was detected, to control the load values. Before the test load of pressure sensors in the universal test machine on the check to determine the demarcation of their value. Examination of the level load by a hydraulic jack on push-pull, and Jack through four bolts in the connector installation of anti-shelf, it can exert the maximum rated load of ± 500 KN, the scope for expansion to ± 300 mm.

3.4 loading

Fig.7 and Fig.8 showed the experimental equipment by which the reciprocating horizontal load is applied to the axial line of the beam in upper story of frame. In experiment, the 80KN vertical loads on steel frame are constant throughout the whole loading. The reciprocating horizontal load is applied in several grades. Before reaching the yield point, an individual specimen was first subjected to two load cycles of 20% the expected yield value, then the load was increased 30KN and the two load cycles was also adopted. When generally close to the yield load, such as reaching that of 60% the ultimate load, the increasement of each grade reduced to about 10% of total load. Before reaching the yield displacement,

used the method below to apply the loads step by step, and each grade repeated once, until the structure was yield. The yield displacement can be determined using the following two ways: a. a cross-section of steel reached the yield strain of specimens which was obtained prior; b. turning point appeared in the P- Δ curve obviously. The load was then increased until the initial beam yielding was recorded by the strain gauges or the apparent turning point was turned out in the curve of connection M- ϕ . Then for subsequent loading cycles, the rotation of connection was incrementally increased by the yield rotation up to the failure of connections. The models of the failure of connections included top and seat angles fracturing, local flections of column flange and the looseness of bolts. In reaching either of failure modes, the test would be terminated. A typical loading routine is presented in Fig.9.

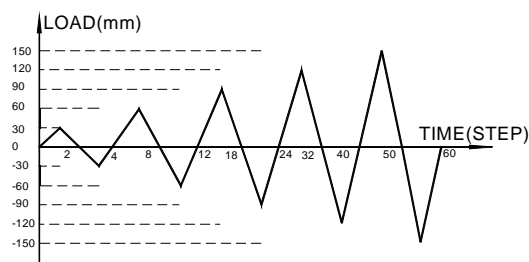


Fig9: actual loading routine of specimens

3.5 Displacement test and rotation angle measurement

The experiment adopted large measuring range strain displacement meter to test the lateral displacement of one-second height of the mid-span beam in the two-story frame, and drew the hysteresis loops of the specimens with horizontal load transducer by xy function recorder. To KJ-1 and KJ-2, two centesimal meters (meter 1 and 2) were disposed on the joints of one story to measure the relative rotation angle. Set centesimal meters (meter 3、4、5、6) on the two ends of the ground beam to monitor the possible slippage and running. Out of the frame plane, four centesimal meters (meter 7、8、9、10) were set on the proper place to test out-plane lateral displacement of the frame. displacement meters (centesimal meter) were Set as shown in Fig.10.

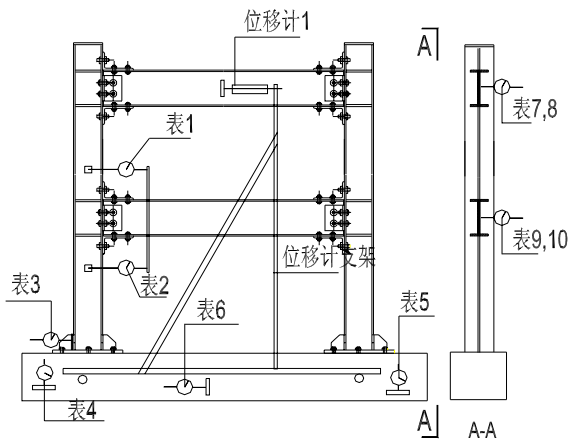


Fig.10 fixing up the displacement meters (centesimal meters)

3.6 Strain test

DH3815 strain gauge was adopted to collect strain value of each part of the steel frame in the course of the loading, the strain gauges were set as Fig.11 shown in detail. The bending moment of frame beams and columns, the time and position plastic hinge appeared were hoped to gain in the test, which can offer basis for applying the horizontal load.

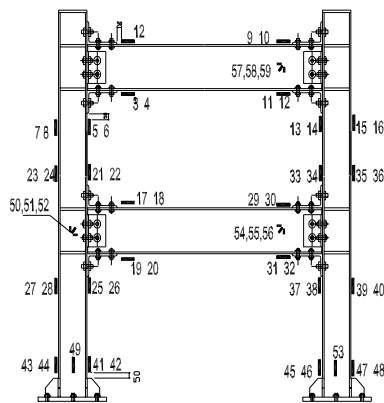


Fig 11 strain gauges KJ-1 and KJ-2 disposing

3.7 Experimental results and discussion

3.7.1 Experimental results

Controlling force and displacement is used in the test. First grading loads was adopted, after reaching to the structural yield load, then follow the multiple of structure yield displacement was applied cyclic loading. Each displacement grade cycle twice, until the structural destroyed. Under the reciprocating horizontal loads of top, the frame model of the test experienced yield, the largest load, and finally some of the load of KJ-2 declined, the destructive load was not gained due to the displacement gauge beyond the range of the restriction. As the lateral drift of the frame KJ-1

and KJ-2 was too large, so the test were terminated. The frame KJ-1 and KJ-2 experienced nine times and eight times repeated cycle of each and finally reached destruction respectively. The final distortion when the test finished was presented in Fig.12. In the test, angle connection appeared greater deformation, as Fig.13 shown. It can be seen in Fig.13 that the top-seat and two web angles connection endured greater deformation under the loads, and some angle connected with column chord was completely divorced from the chord except the position of the bolts, web-angle steel and the surface of column chord nearby also appeared smaller gap.

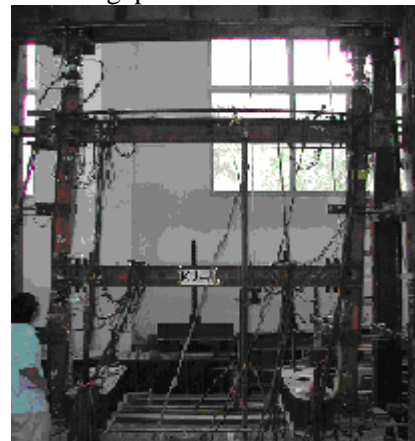


Fig 12 the final form of the frame

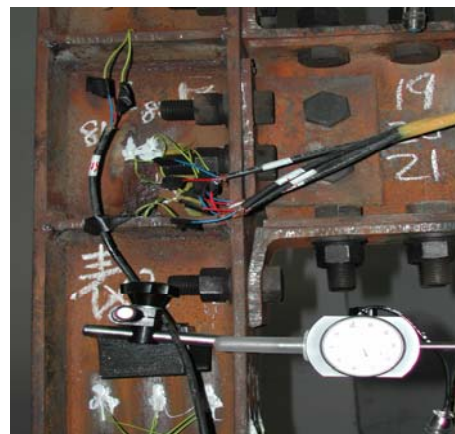
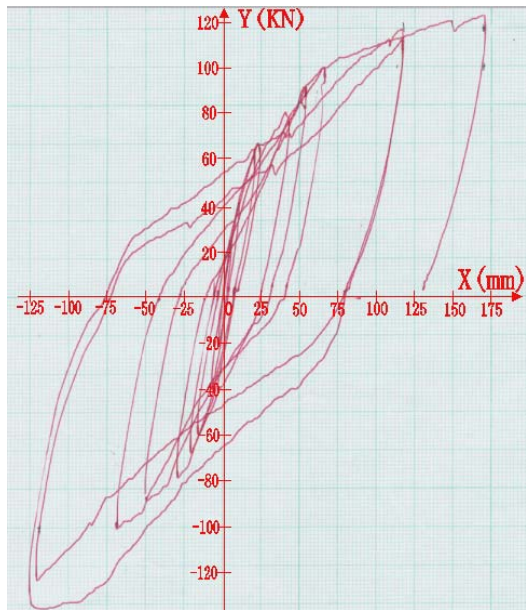
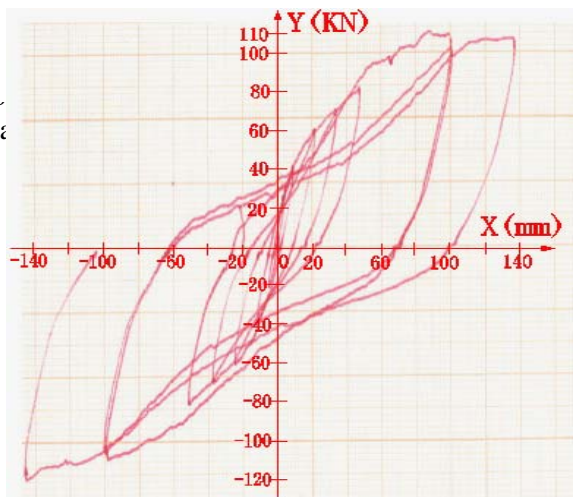


Fig.13 the deformation in angle connection

The load-displacement hysteresis loops of KJ1 and KJ2 are shown as Fig.14. both of hysteresis loops are plump and behave shuttle shape, which demonstrates steel frame structure possesses good property of energy consumption and favorable ductility. Table 4 shows these parameters for some of the tested specimens.



(a) KJ1



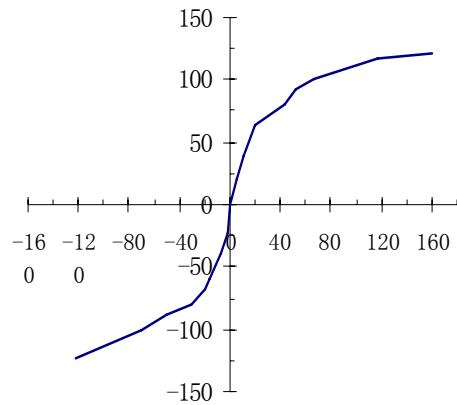
(b) KJ2

Fig.14 load-displacement hysteresis loops of KJ1 and KJ2

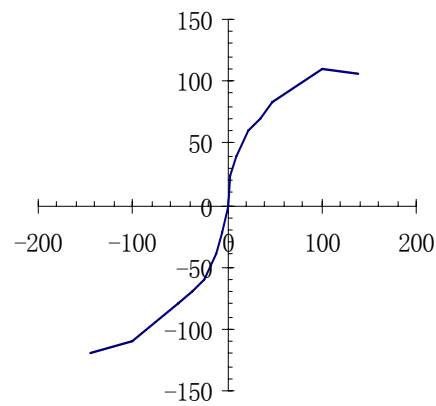
Table 4 some experimental results

Specimen	Yield load (kN)	Yield displacement (mm)	maximum load (kN)	Maximum load (mm)	the ductility coefficient	the initial stiffness (kN/mm)
KJ1	80/-80	43/-30	122/-135	170/-125	3.95/4.16	6.94
KJ2	70/-70	34/-38	110/-120	110/-146	3.2/3.84	5.0

Fig.15 was the envelop of the cyclic response of KJ1 and KJ2 respectively. The relations of moment and rotation were outlined. The line relations of moment and rotation were showed in the initial phase and the phase was very short. With increasing the load, the noalinear relations of moment and rotation became



(a) KJ1



(b) KJ2

Fig .15 Envelope of the cyclic response of specimens

very apparent. The fluctuating phenomenon of the relations was revealed. The main reason was that the In seismic design, cyclic energy dissipation is of great important, since it expresses the ability of the members and their connections to dissipate earthquake input energy. Generally, sufficient energy dissipation without substantial loss of strength and

stiffness constitutes desirable behavior for beam-column subassemblages. It was confirmed that most of the energy was dissipated in the flange of top-seat angles while the column and web angles participated a little in the energy dissipation process in this test.

3.7.2 The analysis of the hysteresis sociality

It can be seen from the hysteresis loops, all the models have better tensility. In actually measured curves, which the frame KJ-1 and KJ-2 of top-seat and two web angles connection were much full, that means their performance of absorbing wre advantage to seismic. According to seismic code, the energy-consuming factor of different kinds of the frame in various stages was calculated, as Table 5 shown. It can be seen from Table 5, From the yielding at begin to the third yield displacement, the energy-consuming factor of the frame was growing, that was to say that of the model frame was growing in a certain range. In addition, the increasing trend of the energy-consuming factor of KJ-2 was obvious, that means the late energy performance of KJ-2 was better. intermediate stage appearing obvious furling phenomena, That was mainly because there was some slippage between the beam chord and connecting angle steel, and the bolts preload minished gradually under the reciprocating loads.

It can be gained from the skeleton curves shown in Fig 6.14, they were not slick, because the gap among linkers, bolts, columns and beams when machining and making the specimens, which can bring certain slippage, and put up dithering on the hysteresis loops and skeleton curves. The linear stage of the two frames KJ-1 and KJ-2 presented was very short in the initial stage of loading, when the loads reached 60KN, non-linearity appeared because of the obvious yield of the connecting angle steel, and result in frame connecting yield when enduring smaller loads.

In the course of loading, according to the test phenomena and strain value gained from the strain gages, much energy that KJ-1 and KJ-2 absorbed was dissipated by the deformation of the connecting angle steel, little was dissipated by the beam and column chord of the connections.

It can be seen From all levels of hysteresis loop diagonal angle decreases, that stiffness of specimens lost after came into the plastic, which was mainly because of the plastic deformation of connected angle and the slippage of high strength bolts in keyhole. This phenomenon has significantly changed the shape of hysteresis loop. According to seismic code, the lateral rigidity of the frame was calculated, and the stiffness curve of the model

frame in every loading stages was drawn. (Fig.16). As can be seen from the Fig.16, the stiffness of KJ-1 and KJ-2 were smaller, and anti-lateral performance were better.

Table 5
dissipation coefficient in every stage

Frame types	dissipation coefficient in every stage					
	yield	$1 \Delta_c^1$	$1 \Delta_c^2$	$2 \Delta_c^1$	$2 \Delta_c^2$	$3 \Delta_c^1$
KJ-1	1.132	1.305	1.602	1.650	-	-
KJ-2	0.96	1.374	1.262	1.401	-	-

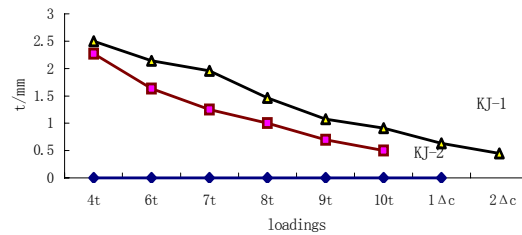


Fig.16 stiffness of the frame

Tensility coefficient is the ratio of the ultimate displacement Δ_u and yield displacement Δ_y when the frame destructed, namely $\mu = \Delta_u / \Delta_y$, and this test did not come to ultimate displacement Δ_u , so there was no tensility coefficient. But the ratio of the largest displacement Δ_{max} and yield displacement Δ_y was as follows shown:

$$\mu \geq \Delta_{max} / \Delta_y = 135 / 20 = 6.75 \text{ (KJ-1)}$$

$$\mu \geq \Delta_{max} / \Delta_y \geq 100 / 22 = 4.54 \text{ (KJ-2)}$$

Seismic Design specifications requires the framework tensility coefficient factor $\mu \geq 4.0$, and it could be obtained that tensility coefficients of two types of steel frame were satisfied. That was to say that the steel frame had good anti-seismic capacity.

3.7.3 Moment and rotation angle analysis

According to two Electrical and Mechanical centesimal meters tables 1 and 2, the rotation angles of beams and columns were calculated. The beam end moments were calculated by analyzing the strain value.

After analysis, the relation between Bending moment and rotation angle can be drawn, as shown in Figure 6.16.

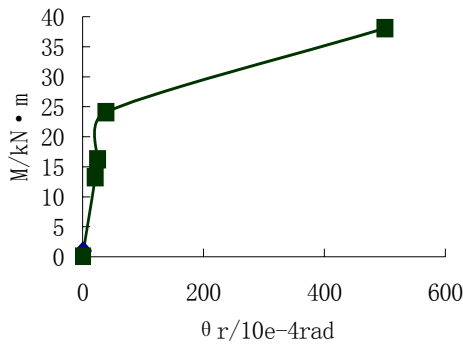


Fig.17 the relation between bending moment and rotation angle

3.7.4 plastic hinge analysis

Because the strain gages could not be pasted on the angles of the semi-rigid connections in KJ-1 and KJ-2, the strain value could not be gained in different loading stages. At the same time, larger deformation of the angles could be observed in the testing, That was to say the angle was more flexible, and making beam ends suffered smaller moment, so there was no plastic hinge appeared on beam ends. According to the yield phenomenon gained from the analysis of strain values, this occurred only in the side-angle chord had also proved this point. Semi-rigid steel frame was difficult to meet the "strong nodes and weak components" of the seismic design requirements. According to the strain gages, the time and order plastic hinges could also be found, as shown in Fig.18. As can be seen from the Fig.18, plastic hinge first appeared in the beam ends, and later in the column ends, which satisfying "strong columns and weak beams" of the design requirements.

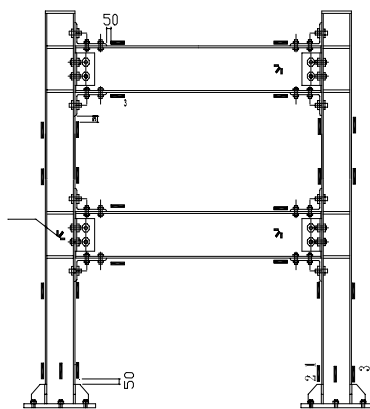


Fig.18 the yield order of each frame in loading stage

4 Finite element analysis

4.1 establishment of finite element model and material parameters

The mode of KJ-1 is established and analyzed by ANSYS. The finite element model of KJ-1 is shown as Fig.19 in which steel frame is divided into beam119 elements.

The stress-strain relation curve of steel is decided by actual testing result of materials. Other material parameters are listed as following: the elastic modulus of steel is $1.9793 \times 105\text{Mpa}$, and the Poisson's ratio of steel is 0.27.

4.2 computation results

Through the finite element computation, the load-displacement hysteresis loops, the curve of load-angle relation of top-seat and two web angles connections, the skeleton curve of load-displacement relation, the curve of degeneration of rigidity, the equivalent stress contours under yield and ultimate loads and other results of KJ1 are obtained here shown in Fig.19-22.

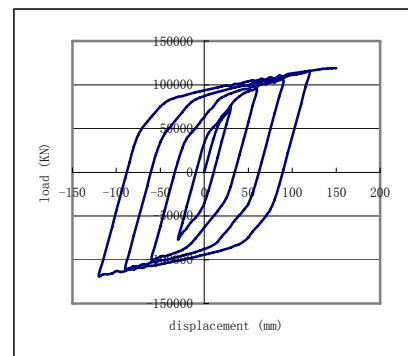


Fig 19 load-displacement hysteresis loops

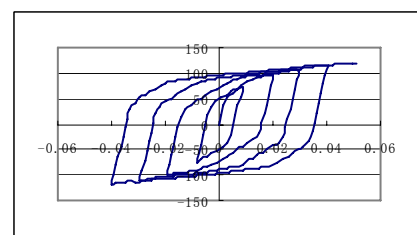


Fig 20 load-angle hysteresis loops

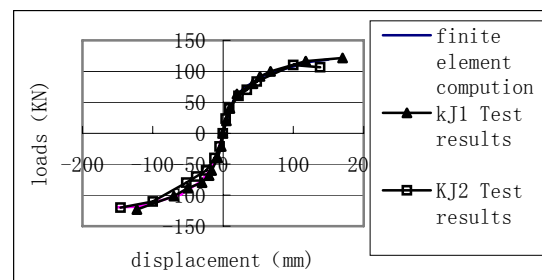


Fig.21 comparison of envelope between finite element and test

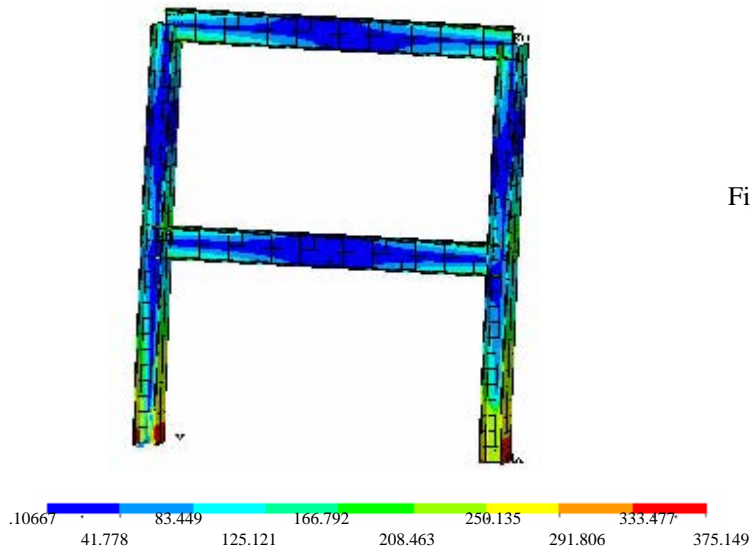


Fig.22 the last deformation figure of steel frame

Fig.19 and Fig.20 demonstrate that the computation results by finite element method accord with the experimental ones well. Because of the limitation of experimental loading equipment, the plastic hinge does not form in frame, so that latter phase of load-displacement curve cannot be got, but the front part coincides with the computation curve very well. Fig 8 also indicates that steel frame with semi-rigid connections can possess the relative high stiffness, strength and excellent ductility, because of the better deformation ability of top-seat and two web angles connections.

Fig.20 shows that envelope curves between finite element computation and test are very similar, so the finite element computation results are reliable.

Figure 10 shows the deformation and equivalent stress contours of frame when horizontal load is increased 115KN. Some results show that the maximum horizontal displacement of beam in upper story of frame is 172.327mm, the maximum stress is 375.149 KN/m². With the increase of load, the plastic area extends to bottom of column, and forms a plastic hinge in bottom of column. At last when a plastic hinge is formed in every bottom of column in frame, the frame becomes a mechanism so the computation is finished, as shown in Fig.23 and Fig.24. This demonstrates that the computation results by finite element method accord with the experimental ones well.

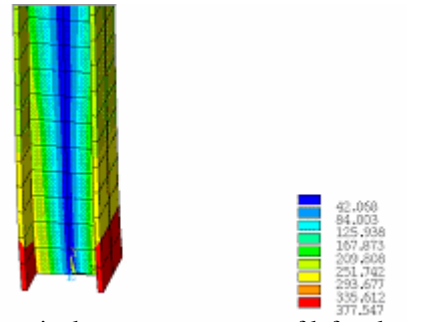


Fig.23 equivalent stress contours of left column bottom under ultimate load

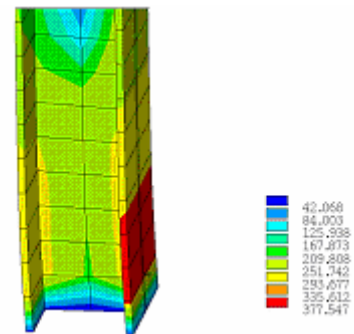


Fig.24 equivalent stress contours of right column bottom under ultimate load

5 Conclusions

It was confirmed that most of the energy was dissipated in the flange of top-seat angles while the column and web angles participated a little in the energy dissipation process in this test.

The experimental research and finite element analysis on steel frame structure with semi-rigid connections show that a significant extent lateral resistant rigidity, ability of energy consumption and ductility of this structural system are better than common steel rigid frame structural system.

References.

- [1]C. Bernuzzi, R. Zandonini and P. Zanon. Experimental analysis and modeling of semi-rigid steel joints under cyclic reversal loading. *Construct. Steel Research*[J], vol.38. February 1996.pp.95 ~ 123,
- [2]E. M. Lui and W-F. Chen, Analysis and behavior of flexibly-jointed frames, *Engineering and Structure*, Vol.8, April, 1986.pp: 107-118
- [3]K.S.Sivakumaran, Seismic response of multi-storey steel buildings with flexible connections, *Engineering and Structure*, Vol.10, October 1988,pp: 239-247
- [4]Hsieh S-H, Deierlein, Nonlinear analysis of three-dimensional steel frames with semi-rigid

connections.Computers and Structures[J], v41(5)
1991, pp:995-1009.

[5]Seung-Eock Kim, Kyung-Won Kang .Large-scale
testing of 3-D steel frame accounting for local
buckling .International Journal of Solids and
Structures [J], V41,(18-19) 2004,pp: 5003-5022.